An HST STIS Observation of VW Hydri at the Exact FUV Onset of an Outburst 1

Edward M. Sion

Department of Astronomy and Astrophysics, Villanova University, 800 Lancaster Avenue, Villanova, PA 19085, USA

edward.sion@villanova.edu

F. H. Cheng

Department of Physics, Shanghai University, 99 Shang-Da Road, Shanghai 200436, P.R. China

cheng3@prodigy.net

Boris T. Gänsicke

Department of Physics, University of Warwick Coventry CV4 7AL, United Kingdom

Boris.Gaensicke@warwick.ac.uk

Paula Szkody

Department of Astronomy, University of Washington, Seattle, WA 98195, USA

szkody@alicar.astro.washington.edu

Received	: accepted	

ABSTRACT

We present an analysis of HST STIS data of VW Hyi that we acquired 14 days after a superoutburst. At the time of our observation the system appears to be going into outburst with the longest wavelengths increasing in flux by a factor of 5 while the shortest wavelengths increase by only a factor of 2. Using the distance of 65 pc, a system inclination angle of 60 degrees and a white dwarf mass of 0.86 M_{\odot} , we carried out model fits involving a white dwarf by itself, an optically accretion disk by itself, a composite model using an optically thick accretion disk and a white dwarf, a two-temperature white dwarf model with a cooler more slowly rotating photosphere and a hotter, rapidly rotating accretion belt and a composite model involving a white dwarf and a rapidly rotating cooler disk ring heated up to a "low" temperature of 13-14,000K. This component of temperature stays fairly constant throughout the HST observations while the area of the disk ring increases by a factor of 12. We see evidence of a delay in the UV emission consistent with the outburst beginning outside of a disk truncation radius.

Subject headings: Stars: Accretion, Dwarf Novae, White Dwarfs, Chemical

Abundances, Individual: VW Hydri

1. Introduction

The dwarf nova VW Hydri is a well-studied SU UMa-type system having both normal and superoutbursts and lying below the cataclysmic variable period gap with $P_{orb} = 0.074$ days (Warner 1995). It is one of several cataclysmic variables in which the underlying white dwarf accreter is exposed during dwarf nova quiescence. These systems offer the prospect of detailed far UV spectroscopic analyzes which have yielded rotation rates, surface temperatures, dynamical masses, and chemical abundances of their accreted atmospheres (Sion 1999; Gänsicke 1999). Previous studies of the white dwarf in VW Hyi revealed its white dwarf has $T_{eff} = 19,000 K$ (Sion et al. 1995a,b), mass $M_{wd} = 0.86 M_{\odot}$ (Sion et al. 1997), a nitrogen to carbon abundance of 4-5 times the solar ratio and early indications of nucleosynthetic abundances from proton-capture reactions (including P, Al, and Mn) greatly elevated above solar in its accreted atmosphere (Sion et al. 1997, 2001) and a rapidly spinning region hotter than the T_{eff} of the white dwarf (Sion et al. 1996; Gänsicke & Beuermann 1996). All of the above characteristics were confirmed by the HST Cycle 8 STIS abundance study of Sion et al. (2001). As part of this study of the white dwarf during quiescence to get a radial velocity curve, our observation fortuitously covered the beginning of the transition into a normal outburst of VW Hydri. In this paper, we report the results of our analysis of this unforeseen event and its implications for understanding the observed behavior of VW Hydri.

¹Based on observations made with the *Hubble Space Telescope*. *HST* is operated by the Association of Universities for Research in Astronomy, Inc., under NASA Contract NAS5-26555

2. Observations

The observations of VW Hydri were obtained on December 10, 2001, starting at 20:28:00 UT, ~ 14 days after the return to optical quiescence following the November 2001 superoutburst. During the STIS observation of VW Hyi, we serendipitously recorded the onset of a normal outburst (up to $\sim 12^{th}$ magnitude) which eventually reached V = 10.1. The instrumental setup used STIS with the FUV-MAMA detectors in ACCUM mode and the $0.2'' \times 0.2''$ aperture. The disperser was the E140M with a center wavelength of 1425Å, a wavelength range of 1140.0 Å to 1735 Å and a total exposure of 9120 seconds. The exposure was subdivided into 19 individual subexposures which accurately record the remarkable changes in the spectrum. The evolution of the spectra is displayed in figure 1. The first seven spectra looked quite similar with roughly the same flux level. The changes began to be noticeable in spectrum 8 when the flux level rose slightly and emission peaks began to appear. These emission regions showed a marked departure from the flux predicted by a single temperature white dwarf model.

The dramatic change during the observation can also be characterized by examining the flux ratios at the short end, middle and long wavelength end of the STIS spectra. To see the largest change, the fluxes at 1160A, 1450A and 1725A are compared for spectra 1 and 19. The flux ratio of spectrum 1 to spectrum 19 at 1160A is only 1.75 while the flux changes at 1450A and 1725A are 5.0 and 4.7 respectively.

This flux behavior suggests the possibility we are seeing the so-called UV delay where the UV flux lags behind the optical by as much as 12 hours or more during the rise to outburst of many dwarf novae (Livio & Pringle 1992). Unfortunately, there is insufficient time resolution in the optical observations at the time of our HST observation to construct an optical light curve for comparison with the FUV light curve. Two days prior to the HST observation, VW Hydri was fainter than V = 13.5 while 1 day after the HST observation,

VW Hyi had risen to V = 10.1, according to the AAVSO archive.

Overall, the line spectrum in this observation has the same strong absorption features and mix of ions as earlier HST FOS and GHRS spectra (Sion et al. 1995a,b, 1996, 1997) of VW Hydri after outburst or superoutburst (e.g. Si II (1260, 1265), Si III (1300), C II (1335), Si IV (1393, 1402), Si II (1526, 1533), with C IV (1548, 1550) in moderately strong emission). The only emission features in the spectra are C IV (1548, 1550) during the early spectra and a feature near 1350A (C II 1335?) which peaks up as the outburst progresses.

2.1. Synthetic Spectral Fitting

The model atmosphere (Hubeny 1988, -TLUSTY), and spectrum synthesis (Hubeny et al. 1994; Hubeny & Lanz 1995, -SYNSPEC) codes and details of our χ^2 minimization fitting procedures can be found in Sion et al. (1995a,b) and Huang et al. (1996) and for the sake of brevity will not be repeated here. We fixed the distance of VW Hyi at d = 65 pc, fixed the white dwarf radius at $R_{wd} = 9.8 \times 10^{-3} R_{\odot}$, corresponding to the gravitational redshift mass $M_{wd} = 0.86 M_{\odot}$ (Sion et al. 1997). Taking the fixed gravity log g = 8.5 we created white dwarf models for temperatures T/1000 = 14 - 23.5 K in steps of 0.5, rotational velocities $V_{rot} = 200 - 700$ km/s in steps of 100 km/s and chemical abundances Si = 0.1,

Table 1. FUV Flux Variation

Obs.No.	Flux (1160) $<$ erg/s/cm ² /Å>	Flux (1450) $<$ erg/s/cm ² /Å>	Flux (1725) $\langle \text{erg/s/cm}^2/\text{Å} \rangle$	1160	1450	1725
1 19	2.0×10^{-13} 3.5×10^{-13}	2.0×10^{-13} 1.0×10^{-12}	1.5×10^{-13} 7.0×10^{-13}	1.8	5.0	4.7

0.2, 0.3, 0.4, 0.5 x solar abundance, and C = 0.3, 0.4, 0.5, 0.6, 0.7 x solar abundance with all other elements at their solar values initially. This initial grid comprised a total of 3000 models. The white dwarf models have been normalized to a solar radius and a distance of 1 kpc. The model fluxes are scaled to the observed fluxes through the scale factor $S = 4 \times \pi (R_{wd}^2/D^2)$. For the disk models, we made use of the entire parameter space covered by the optically thick accretion disk model grid of Wade & Hubeny (1998) for \dot{M} but held the disk inclination and the white dwarf mass fixed as above. Our accretion belt models were constructed in the same manner as described in Sion et al. (1996). A detailed discussion of the accretion belt models can also be found in Sion et al. (2001).

First, we applied the single temperature white dwarf models to the data. The temperature remained roughly constant (within the uncertainties of T) through spectrum 8 but subsequent observed spectra revealed large changes in the flux level longward of 1600A and relatively small changes in the flux level at shorter wavelengths down to around Lyman Alpha. None of the model fits are successful in a statistical or a qualitative sense. Therefore, the term "best-fitting" refers to the lowest χ^2 value found for each of the 19 spectra. The "best-fitting" white dwarf models to spectra 1 and 19 are displayed in figure 2 and 3. At the beginning of the exposure $T_{eff} = 24,000$ K, $V \sin i = 600$ km/s with $\chi^2 = 15.1767$ while for spectrum 19, $T_{eff} = 32,000$ K, $V \sin i = 600$ km/s with $\chi^2 = 445.953$.

Second, we tried optically thick accretion disk models alone without any white dwarf photospheric radiation contribution. There is very little qualitative improvement apparent and the disk fits, like the photosphere fits, agree very poorly with the observations. Likewise for two-temperature white dwarf models (photosphere plus hotter equatorial belt), the fits are similarly unsatisfactory as they do not account for the long wavelength flux increase. The size and variation of the χ^2 values are very similar to those obtained for the single-temperature photosphere fits.

Clearly, none of the above fitting experiments provided agreement, either qualitatively or quantitatively, with the STIS observations. In view of this failure and the fact that the longward continuum rises while the Lyman Alpha region remains relatively unchanged, we explored the possibility of a cool accretion ring existing around the white dwarf.

We created a grid of white dwarf plus cool accretion disk ring models with the white dwarf temperature, disk ring temperature, disk ring gravity, disk ring velocity, and disk ring area as free parameters. The system distance, white dwarf gravity and rotational velocity, were kept fixed. The chemical abundances of the white dwarf were also kept fixed at the solar values. We let the white dwarf temperature vary between 18 and 28,000K in steps of 1000K. The trial temperatures of the ring were 12,000K, 13,000K, 14,000K and 15,000K, the trial ring velocities were 3400 km/s, 2500 km/s, 1500 km/s and 1000 km/s, the chemical abundance of the ring was kept fixed at the solar values. The ratio of the surface area of the ring to the surface area of the white dwarf was varied from 0.5 to 100 in steps of 0.5.

When a white dwarf model is combined with a cooler accretion ring, this results in a very significant improvement in the quality of the fits. In the spectrum of the undisturbed white dwarf, the flux at 1160A is normally higher than the flux at 1725A. Starting approximately with spectrum 5, the flux at 1725A first starts to surpass the flux level at the shortest wavelength, 1160A. To illustrate the improvement in fitting the evolution of the spectra, it is illuminating to compare spectrum 5 with spectrum 19. In figure 4, the best-fitting composite ring model to spectrum 5 is displayed. For comparison, the best-fitting composite ring model is displayed for spectrum 19 in figure 5. While the fits are far from perfect, they do reproduce the overall spectral shape recorded with STIS. The only discrepancy remaining is that the continuum seems lower than that observed in the 1450-1600A region and some of the absorption lines are not well fit in that region. From the fitting of the evolution of the spectra, we see that the white dwarf temperature

appears to increase from 21,000k to 27,000K. This temperature change is of the same order as the change in temperature of the white dwarf in U Gem in response to its outburst. The temperature of the rotating ring changed only insignificantly, from 14,000 to 13,000K, however the area of the rotating ring, relative to the area of the white dwarf, increased by a factor of 12!

3. Conclusions

The rapid flux increase during the course of the observation starting with spectrum 5 and reaching a peak flux of 1×10^{-12} ergs/cm²/s appears to mark the actual FUV onset of a normal outburst of VW Hyi. The fact that the spectral energy distribution during the marked increase in flux undergoes a substantially larger change at longer UV wavelengths suggests that the outburst began in the outer part of the disk. If the disk is not truncated, then the shape of the overall flux suggests an outside-in type outburst. If however the disk is truncated, then all we can say is that the outburst began external to the truncation radius.

The evolution of the spectrum is surprisingly well-represented by a white dwarf which is being heated at the time of the observation and a rapidly rotating accretion ring, cooler than the white dwarf and expanding in surface area. The greatest change in the STIS spectrum occurs longward of Lyman Alpha suggesting that the events in the disk have not yet fully affected the white dwarf. We have found that the overall evolution of the distribution of spectral energy is well-represented by a white dwarf and a cooler accretion ring of increasing area as the outburst proceeds and of much larger surface area than the white dwarf. We see evidence of a delay in UV emission consistent with outburst beginning outside of a disk truncation radius. While the sparse optical coverage versus time during the HST exposure disallows a detailed comparison with the temporal variation of the FUV

flux, the evolution of the STIS spectra suggest that the UV emission from the white dwarf is delayed relative to the optical rise. If the disk is truncated, then this delay is probably caused by the time it takes viscous diffusion inside the disk truncation radius to fill in the truncated region with gas and reach the white dwarf.

This work is supported by NASA through grants GO8139.01-97A from the Space Telescope Science Institute, which is operated by the Association of Universities for Research in Astronomy, Inc., under NASA Contract NAS5-26555. Support was also provided in part by NSF grant 99-01195 and NASA ADP grant NAG5-8388. BTG was supported by a PPARC Advanced Fellowship.

REFERENCES

Huang, M., Sion, E.M., Hubeny, I., Cheng, F.H., & Szkody, P. 1996, ApJ, 458, 355

Gänsicke, B.1999, ASP Conf.Ser.,169, 315

Gänsicke, B., & Beuermann, K. 1996, A&A, 309, L47

Hubeny, I. 1988, Comput. Phys. Comm., 52, 103

Hubeny, I., & Lanz, T. 1995, ApJ, 439, 875

Hubeny, I., Lanz, T., & Jeffrey, S. 1994, Newsletter on Analysis of Astronomical Spectra (St. Andrews Univ.), 20, 30

Livio, M. & Pringle, J.1992, MNRAS, 259, 23

Sion, E. M. 1999, PASP, 111, 532

Sion, E.M., Szkody, P.Cheng, F.H., & Huang, M. 1995a ApJ, 444, L97

Sion, E.M., Huang, M., Szkody, P., & Cheng, F.H. 1995b ApJ, 445, L31

Sion, E.M., Cheng, F., Huang, M., Hubeny, I., & Szkody, P. 1996, ApJL, 471, L41

Sion, E.M, Cheng, F., Sparks, W.M., Szkody, P., Huang, M., & Hubeny, I. 1997, ApJL, 480, L17

Sion, E.M., Cheng, F., Szkody, P., Gänsicke, B., Sparks, W.M.2001, ApJ,

Wade, R.A., & Hubeny, I. 1998, ApJ, 509, 350

Warner, B. 1995, Cataclysmic Variable Stars, (Cambridge, GB: Cambridge University Press)

Figure Captions

Figure 1: The sequence of 19 ACCUM spectra from the start to the finish of the 10 December, 2001 STIS observation. Note the dramatic changes in the spectrum from the beginning to the end of the exposure.

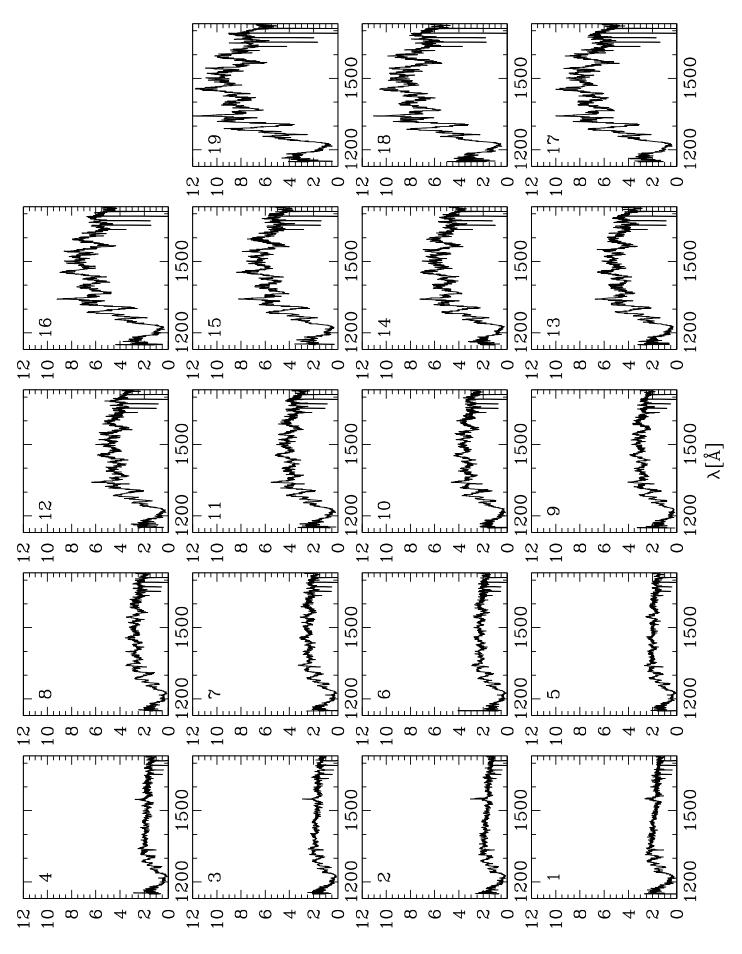
Figure 2: The best fit synthetic spectrum of a white dwarf alone, to spectrum $1, \sim 14$ days post-superoutburst. ($T_{eff} = 24,000$ K, $\log g = 7.5$, $V_{sin} = 600$ km/s, Si abundance 0.5 solar, C abundance 1.0 solar (see text for details);

Figure 3: The best fit synthetic spectrum of a white dwarf alone, to spectrum $19, \sim 14$ days post-superoutburst. ($T_{eff} = 32,000$ K, $\log g = 8.5$, $V_{sin} = 600$ km/s, Si abundance 0.2 solar, C abundance 0.1 solar (see text for details);

Figure 4: The best-fitting composite white dwarf plus rotating ring model to spectrum 5. The white dwarf has $T_{eff} = 21{,}000\text{K}$ and provides 64% of the light while the rotating ring has $T_{ring} = 14{,}000\text{K}$, $\log g = 6$, $V_{ring} = 3400 \text{ km/s}$ and provides 36% of the light. The dotted line is the white dwarf synthetic flux, the dashed line is the ring synthetic flux and the solid line is the combined flux of the two components.

Figure 5: The best-fitting composite white dwarf plus rotating ring model to spectrum 19. The white dwarf now has $T_{eff} = 27,000$ K and provides 36% of the light while the rotating ring has $T_{ring} = 13,000$ K, log g = 7, $V_{ring} = 1500$ km/s and provides 64% of the light. The dotted line is the white dwarf synthetic flux, the dashed line is the ring synthetic flux and the solid line is the combined flux of the two components.

This manuscript was prepared with the AAS LATEX macros v5.2.



 $\mathbf{E}^{y} \; \left[\, \mathbf{10}_{-13} \mathrm{erg} \; \mathrm{cm}_{-1} \mathrm{z}_{-1} \mathbf{y}_{-1} \right]$

